The Clinical Phenotype of *CNGA3*-Related Achromatopsia: Pretreatment Characterization in Preparation of a Gene Replacement Therapy Trial

Ditta Zobor,[1] Annette Werner,[1] Franco Stanzial,[2] Francesco Benedicenti,[2] Günther Rudolph,[3] Ulrich Kellner,[4] Christian Hamel,[5] Sten Andréasson,[6] Gergely Zobor,[1] Torsten Strasser,[1] Bernd Wissinger,[1] Susanne Kohl,[1] and Eberhart Zrenner[1,7]; for the RD-CURE Consortium

[1]Center for Ophthalmology, University of Tübingen, Tübingen, Germany
[2]Department of Pediatrics, Genetic Counseling Service, Hospital of Bolzano, Bolzano, Italy
[3]Department of Ophthalmology, Ludwig-Maximilians-University, Munich, Germany
[4]Rare Retinal Disease Center, AugenZentrum Siegburg, Siegburg, Germany
[5]Institute of Neurosciences of Montpellier, Hôpital Saint Eloi, Montpellier, France
[6]Department of Ophthalmology, Lund University, Lund, Sweden
[7]Werner Reichardt Center for Integrative Neuroscience, University of Tübingen, Tübingen, Germany

Correspondence: Ditta Zobor, Institute for Ophthalmic Research, University of Tübingen, Schleichstr. 12-16, D-72076 Tübingen, Germany; ditta.zobor@uni-tuebingen.de.

SK and EZ are joint senior authors.

See the appendix for the members of the RD-CURE Consortium.

Submitted: July 31, 2016
Accepted: January 2, 2017

Citation: Zobor D, Werner A, Stanzial F, et al.; for the RD-CURE Consortium. The clinical phenotype of *CNGA3*-related achromatopsia: pretreatment characterization in preparation of a gene replacement therapy trial. *Invest Ophthalmol Vis Sci*. 2017;58:821–832. DOI:10.1167/iovs.16-20427

Purpose. The purpose of this study was to clinically characterize patients with *CNGA3*-linked achromatopsia (CNGA3-ACHM) in preparation of a gene therapy trial.

Methods. Thirty-six patients (age 7–56 years) with complete (cACHM) or incomplete (iACHM) CNGA3-ACHM were examined, including detailed psychophysical tests, extended electrophysiology, and assessment of morphology by fundus autofluorescence and spectral-domain optical coherence tomography (SD-OCT).

Results. Mean best-corrected visual acuity was 0.78 ± 0.14 logMAR. Color vision tests were consistent with a rod-dominated function in every cACHM patient. Microperimetry indicated an overall lowered retinal sensitivity within 20° of visual field. In electroretinography (ERG), photopic responses were nondetectable in cACHM patients, but residual cone responses were observed in the iACHM patients. Scotopic responses were altered referring to anomalies of photoreceptor and postreceptor signaling, whereas in voltage versus intensity functions, V_{max} was significantly below normal values ($P < 0.05$). In contrast, slope (n) and semisaturation intensity (K) were found to be within normal limits. Spectral-domain OCT examination showed no specific changes in 14.7%, disruption of the ellipsoid zone (EZ) at the fovea in 38.2%, absent EZ in 17.7%, a hyporeflective zone in 20.5%, and outer retinal atrophy in 8.9% of all cases and foveal hypoplasia in 29 patients (85%). No correlation of retinal morphology with visual function or with a specific genotype was found. The severity of morphologic and functional changes lacked a robust association with age.

Conclusions. Our extended investigations prove that even among such a genetically homogenous group of patients, no specific correlations regarding function and morphology severity and age can be observed. Therefore, the therapeutic window seems to be wider than previously indicated.

Keywords: achromatopsia, *CNGA3*, genotype–phenotype, gene therapy

Achromatopsia (ACHM) is a rare autosomal recessive inherited retinal disorder with an incidence of approximately 1 in 30,000. It presents shortly after birth or early infancy and is typically characterized by reduced visual acuity, nystagmus, photophobia, and very poor or absent color vision. The clinical diagnosis of ACHM is based on the typical symptoms supported by morphologic and functional, especially electrophysiologic, findings, which typically show absent or markedly reduced cone responses, whereas rod responses are normal or nearly normal.[1,2] However, deficits in rod and rod-mediated function have also been demonstrated.[3] Achromatopsia can be caused by mutations in the *CNGA3, CNGB3, GNAT2, PDE6C*, and *PDE6H* genes,[4–12] all of which encode components of the cone phototransduction cascade. Recently, *ATF6* has been identified as a new ACHM gene, suggesting a crucial and unexpected role of ATF6A in human foveal development and cone function.[13]

There have been several clinical studies in recent years focusing on retinal architecture and foveal morphology in detail by using high-resolution optical coherence tomography (OCT) and adaptive optics (AO) in patient cohorts with mutations in several of the known ACHM-associated genes.[14–21] Although ACHM is considered a functionally nonprogressive disease affecting only the cone photoreceptor system, studies have described slow, age-dependent changes in the retinal architecture[16,17]: an observation that is corroborated by the analysis of the corresponding animal models.[22–25] On the contrary, Genead et al. provided evidence that cone loss is not age

dependent.[26] Although retinal structure seems to show great variability and slow progressive cone loss has been suggested, interestingly, no clear association between retinal structure and function could be described.[15]

The purpose of the present study was to summarize the clinical functional and morphologic findings observed in CNGA3-related ACHM patients to determine whether there are special characteristics of such a genetically homogenous group, whether we can obtain further genotype–phenotype correlations, and also to experience which tests will be most suitable for the interventional study phase. To the best of our knowledge, this reported prospective study describes the largest thoroughly investigated group of on CNGA3-ACHM patients. Furthermore, four novel mutations are reported here for the first time.

Subjects and Methods

All examinations were carried out in accordance with the Declaration of Helsinki. The study was approved by the Ethics Committee of the Medical Faculty of University of Tübingen, and patients gave prior written informed consent.

The subjects underwent a detailed clinical history and complete ophthalmologic examination including psychophysical tests (visual acuity, color vision, contrast sensitivity, visual field, microperimetry, and dark adaptation) and extended electrophysiology (full-field and multifocal electroretinography [ERG]).

Psychophysical Tests

Best-corrected visual acuity (BCVA) was assessed with the Early Treatment Diabetic Retinopathy Study (ETDRS) chart. Contrast sensitivity was measured with the Pelli Robson chart at 1 m. Visual field tests were performed using an Octopus 900 perimeter (Haag-Streit International, Wedel, Germany). Semi-automated kinetic perimetry was carried out using Goldmann stimuli III4e, I4e, and additional dimmer stimuli, where possible, within the 90° visual field and automated static perimetry within the 30° visual field.

Color vision tests were performed with both the Rayleigh anomaloscope (Oculus GmbH, Wetzlar, Germany) and the Roth 28 Hue saturated test (Richmond Products, Inc., Albuquerque, NM, USA) in each patient. Additionally, we investigated color discrimination by means of the computer-based Cambridge Color Test (CCT; Cambridge Research Systems, Rochester, UK)[27] in four study patients (Supplementary Data S1; Supplementary Fig. S1).

Microperimetry was performed after pupil dilatation using the MP-1 microperimeter (Nidek Technologies, Padova, Italy) (Supplementary Data S2).

Dark adaptation thresholds were measured with the full-field stimulus threshold (FST) test of the Diagnosys Espion system with the ColorDome LED full-field stimulator and button box (Diagnosys LLC, Lowell, MA, USA) for short (FST blue, 465 nm) and long wavelength stimuli (FST red, 635 nm) after 30-minute adaptation time to isolate rod and cone adaptation thresholds. The protocol by Klein and Birch was used for FST testing.[28,29]

Electrophysiology

Full-field and multifocal ERGs were recorded according to the standards of the International Society for Clinical Electrophysiology of Vision (ISCEV),[30,31] but additional stimuli were included to improve retinal function evaluation. The stimulus-response function was fitted to scotopic ERG amplitudes to derive the response maximum V_{max}, the slope n, and the log retinal illuminance that produces the half-maximum response, K (Supplementary Data S3).

Morphologic Examinations

For detailed morphologic examination, fundus photography, fundus autofluorescence (FAF), and spectral-domain OCT (SD-OCT) recordings (Heidelberg Engineering GmbH, Heidelberg, Germany) were performed in every patient after pupillary dilation.

Horizontal and vertical OCT scans (9 mm) through the fovea and, where possible, volume scans (37 B-scan, 20° × 20°) using the automatic real-time (ART) software were acquired. Foveal structure of SD-OCT images was graded into five categories according to Sundaram et al.[15]: (1) continuous inner segment ellipsoid zone (EZ), (2) EZ disruption, (3) absence of EZ, (4) presence of a hyporeflective zone (HRZ), and (5) outer retinal atrophy including RPE loss. Furthermore, retinal structure of the fovea was also analyzed to determine the presence or absence of foveal hypoplasia.[32] Finally, central retinal thickness (CRT) was calculated.

Genetic Analysis

Details about the genetic analysis of patients can be found in Supplementary Data S4.

Statistical Analysis

The statistical analysis of the data was conducted using the JMP 11 statistical software (SAS Institute, Cary, NC, USA). Normality of data was assessed by evaluation of the histogram plots, and correlation parameters were calculated using Pearson or Spearman analysis, where appropriate. The dominant eye was noted in the patient history, and correlations between the dominant and contralateral, as well as between the right and left eye, were assessed. The dominant eye was selected for further analysis.

Results

Twelve female and 24 male subjects (mean age, 33.7 years; range, 7–56 years) from 30 families were included. Their clinical and genetic findings are summarized in Table 1. Patients older than 18 years of age were recruited for the clinical screening in preparation to a gene therapy trial, but results of two younger siblings were also included here to see a wider age spectrum of the phenotype.

Genetic Results

Within the cohort, 18 patients carried a homozygous mutation and 18 patients carried two heterozygous mutations in *CNGA3* (Table 1). Compound heterozygosity was confirmed by family segregation analysis in 7 cases, and true homozygosity for the observed *CNGA3* mutation was confirmed in 11 cases. Most mutations have already been published, but four (c.1682G>A;p.G561E, c.139C>T;p.Q47*, c.784G>C;p.A282P, c.1116delC;p.V373*) represent novel mutations reported herein for the first time (Fig. 1; Table 1).

In 14 patients, all coding exons of *CNGB3* were also sequenced. In two patients (RD008 and RD017), additional mutations and variants were hereby identified. Patient RD008 is homozygous for *CNGA3* c.1529G>C;p.C510S. This mutation affects a highly conserved amino acid residue in the cGMP-binding domain and has never been observed in various databases including the ExAc Browser. In our cohort, it is

Table 1. Clinical Characteristics and Genetic Findings of *CNGA3*-ACHM Patients

Patient No.	Age, y	Ethnicity	Sex	*CNGA3* Genotypes		Clinical Phenotype	BCVA logMAR		OCT Category		Foveal Hypoplasia	
				Nucleotide Sequence	Protein Sequence		OD	OS	OD	OS	OD	OS
RD001	24	German	M			cACHM	1	0.9	4	4	Yes	Yes
RD002	40	German	F	c.800G>A/c.1963C>T	p.G267D/p.Q655*	cACHM	1	1	1	1	No	No
RD003	37	German	M	c.800G>A/c.1963C>T	p.G267D/p.Q655*	cACHM	0.9	0.9	1	1	Yes	Yes
RD004	56	German	M	c.544A>T/c.1641C>A	p.N182Y/**p.F547L**	iACHM	0.7	0.7	3	3	Yes	Yes
RD005	52	German	F	c.872C>G/c.1641C>A	**p.T291R/p.F547L**	cACHM	0.8	0.9	2	1	Yes	Yes
RD006	41	Turkish	M	c.1641C>A/*c.1682G>A*	**p.F547L**/*p.G561E*	cACHM	0.9	0.7	5	5	Yes	Yes
RD007	43	German	M	c.829C>T/c.1687C>T	p.R277C/**p.R563C**	iACHM	0.9	0.8	3	2	No	No
RD008†	41	German	M	c.1529G>C/c.1529G>C	p.C510S/p.C510S	cACHM	0.8	0.8	3	3	Yes	Yes
RD009	18	Italian	M	c.847C>T/c.847C>T	p.R283W/p.R283W	cACHM	0.8	0.8	3	2	Yes	Yes
RD010	43	Italian	F	c.847C>T/c.847C>T	p.R283W/p.R283W	cACHM	0.9	0.7	4	4	Yes	Yes
RD011	18	Italian	F	c.847C>T/c.847C>T	p.R283W/p.R283W	cACHM	1	0.9	4	4	Yes	Yes
RD012	27	Italian	M	c.847C>T/c.847C>T	p.R283W/p.R283W	cACHM	0.7	0.8	3	3	Yes	Yes
RD013	27	German	M	c.1641C>A/c.778G>A	**p.F547L**/p.D260N	cACHM	0.7	0.6	1	1	Yes	Yes
RD014	39	Italian	M	c.847C>T/c.847C>T	p.R283W/p.R283W	cACHM	0.8	0.9	1	2	Yes	Yes
RD015	54	German	M	*c.139C>T*/c.1495C>T	*p.Q47**/p.R499*	cACHM	0.8	0.7	3	3	Yes	Yes
RD016	22	Italian	M	c.1538G>A/c.1706 G>A	p.G513E/p.R569H	cACHM	1	1	2	2	Yes	Yes
RD017‡	54	German	F	c.661C>T/c.829C>T	p.R221*/p.R277C	cACHM	0.7	0.6	4	4	Yes	Yes
RD018	52	German	M	c.1641C>A/c.1641C>A	**p.F547L/p.F547L**	cACHM	0.9	0.9	5	5	Yes	Yes
RD019	37	Italian	M	c.848G>A/c.848G>A	**p.R283Q/p.R283Q**	cACHM	0.8	0.9	2	2	No	No
RD020	35	Austrian	F	c.830G>A/c.1706G>A	p.R277H/p.R569H	cACHM	0.7	0.7	4	4	Yes	No
RD021	45	Austrian	F	c.667C>T/c.830G>A	p.R223W/p.R277H	cACHM	0.6	0.6	4	4	Yes	Yes
RD022	46	German	F	c.1641C>A/c.1641C>A	**p.F547L/p.F547L**	cACHM	0.7	0.6	1	1	Yes	Yes
RD023	26	Italian	M	c.940_942delATC/c.940_942delATC	p.I314del/p.I314del	cACHM	0.8	0.9	2	2	Yes	Yes
RD024	48	German/Turkish	M	*c.784G>C*/c.1641C>A	*p.A262P*/**p.F547L**	iACHM	1	0.9	2	2	Yes	Yes
RD025	50	German	F	c.1306C>T/c.1306C>T	p.R436W/p.R436W	cACHM	0.7	0.6	2	2	Yes	Yes
RD026	37	Indian	M	c.1641C>A/c.1641C>A	**p.F547L/p.F547L**	cACHM	0.7	0.9	5	5	No	No
RD027	35	Indian	F	c.1641C>A/c.1641C>A	**p.F547L/p.F547L**	cACHM	0.9	0.8	1	2	Yes	Yes
RD028	18	German	M	c.1443dupC/c.1642G>A	p.I482Hfs*6/p.G548R	cACHM	0.8	0.9	2	3	Yes	Yes
RD029	22	Arab	M	c.829C>T/c.829C>T	p.R277C/p.R277C	cACHM	0.8	0.9	3	2	Yes	No
RD030	28	Arab	M	c.829C>T/c.829C>T	p.R277C/p.R277C	cACHM	0.6	0.7	3	2	Yes	No
RD031	22	Swedish	M	c.847C>T/c.847C>T	p.R283W/p.R283W	cACHM	0.7	0.7	3	2	Yes	Yes
RD032	18	French	F	*c.1116delC*/c.1579C>A	*p.V373**/p.L527M	cACHM	0.8	0.8	1	1	Yes	Yes
RD033	11	Italian	M	c.847C>T/c.847C>T	p.R283W/p.R283W	cACHM	0.9	0.9	1	2	Yes	Yes
RD034	7	Italian	M	c.847C>T/c.847C>T	p.R283W/p.R283W	cACHM	1	1	4	4	Yes	Yes
RD035	18	German	M	c.1279C>T/c.1641C>A	p.R427C/**p.F547L**	iACHM	1	1	n.a.	n.a.	n.a.	n.a.
RD036	24	German	F	c.671C>G/c.1106C>G	p.T224R/**p.T369S**	iACHM	0.4	0.4	2	2	No	No

In vitro electrophysiologic findings presume remaining channel activity in some of the mutations (in bold); however, not in every case could remaining cone function be detected. In contrast, not all iACHM patients harbored mutations, where residual cone could be expected from functional in vitro studies. Patients RD002 and RD003, RD009 and RD033, RD011 and RD034, RD026 and RD027, and RD029 and RD030 were siblings, whereas RD010 and RD012 were first-degree cousins. New mutations are written in italics. F, female; M, male; n.a., not available; OD, right eye; OS, left eye.

† Additional mutation: c.1204G>T p.V402F homozygous in the *CNGB3* gene.

‡ Additional mutation: c.886_896 del11insT; p.R296fs* heterozygous in the *CNGB3* gene.

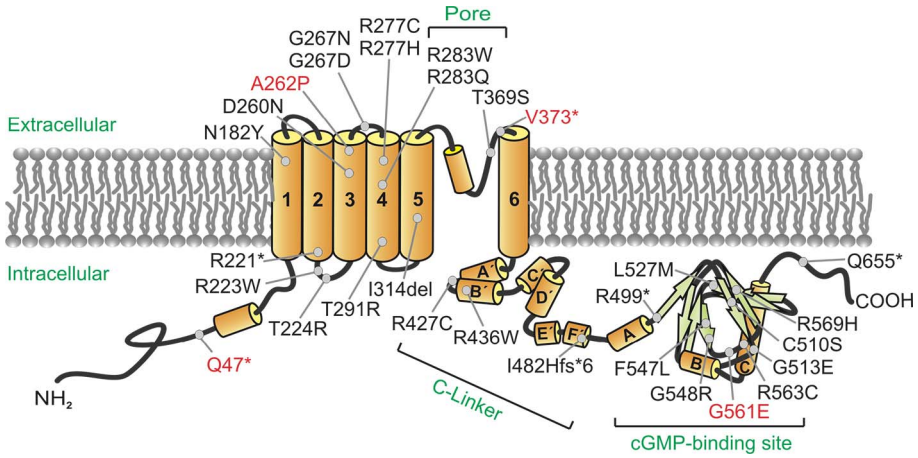

Figure 1. Structure of the α subunit of the cone photoreceptor cGMP-gated cation channel encoded by the *CNGA3* gene and mutations detected in our patient cohort. New mutations are written in red.

private to this patient. The mutation has been tested functionally in a heterologous expression system and was shown to lead to complete function loss of the respective homomeric CNGA3 channel.[33] In addition, we found this patient to be also homozygous for *CNGB3* c.1204G>T;p.V402F (rs139825253). This variant is conserved between CNGB3 and CNGB1 polypeptides and localizes to the pore helix. However, as it was observed heterozygously in 56/120.852 alleles in the ExAc Browser, we consider it more likely a rare benign variant than a pathogenic mutation. Patient (RD017) carries two heterozygous mutations in *CNGA3* c.661C>T;p.R221* and c.829C>T;p.R277C. As c.661C>T;p.R221* is a nonsense mutation, it is considered pathogenic. The second mutant allele c.829C>T;p.R277C is again a missense mutation, affecting a highly conserved amino acid residue in transmembrane domain S4. It is a rather common mutation in *CNGA3*-ACHM and has also been functionally characterized.[33] In addition, this patient is heterozygous for *CNGB3* c.886_896delinsT;p.T296Yfs*9, which is an indel mutation resulting in a frameshift and premature stop codon and therefore is also considered a true mutation. However, no other *CNGB3* mutant allele was identified in this patient. Therefore, we consider the *CNGA3* mutations primarily causative for ACHM in RD017, although we cannot rule out or neglect a contribution of the heterozygous deleterious *CNGB3* allele on the disease presentation in this patient.

Psychophysical Tests

In five cases, incomplete ACHM (iACHM) was diagnosed based on the clinical findings of electrophysiologic tests,[1,2] whereas 31 patients presented with complete ACHM (cACHM). In one iACHM patient (RD036), the remaining cone function resulted in considerably better clinical results (i.e., BCVA, color vision, ERG), whereas the other four iACHM patients only showed reproducible, but severely reduced, 31-Hz flicker responses of the photopic ERG in the Fourier analysis. Other clinical parameters of these four iACHM (RD004, RD007, RD24, and RD035) cases did not differ from cACHM; therefore, only the patient with the clearly better cone function was excluded from further analysis. Mean BCVA was 0.78 ± 0.14 logarithm of the minimal angle of resolution (logMAR) (range, 0.6–1

Table 2. Comparison (Paired *t*-Test) of Functional and Morphologic Results Between the Dominant and Nondominant Eye and Between iACHM and cACHM Patients

Clinical Parameters	Dominant Eye (n = 35), Mean ± SD	Nondominant Eye (n = 35), Mean ± SD	df	t Value	P Value	Correlation r	iACHM (n = 4), Mean ± SD	cACHM (n = 30), Mean ± SD
BCVA, logMAR	0.78 ± 0.14	0.83 ± 0.13	16	−3.0958	**0.0069****	**0.84**	0.76 ± 0.23	0.78 ± 0.12
Contrast sensitivity, logCS	1.21 ± 0.2	1.11 ± 0.27	16	3.0499	**0.0076****	**0.87**	1.05 ± 0.21	1.23 ± 0.18
Color confusion, CCI	5.22 ± 0.58	5.34 ± 0.97	16	−1.8856	0.07	0.24	5.21 ± 0.42	5.15 ± 0.55
Anomaloscope slope, SQ	−1.60 ± 0.27	−1.58 ± 0.28	16	−0.2889	0.77	0.54	−1.39 ± 0.23	−1.62 ± 0.27
MP1 mean sensitivity, dB	15.08 ± 2.37	14.39 ± 2.88	16	0.6803	0.50	0.6	17.3 ± 0.65	14.91 ± 2.37
FST blue, dB	−56.17 ± 5.85	−55.70 ± 5.36	16	−1.3967	0.18	**0.69**	−53.61 ± 6.64	−56.45 ± 5.83
FST red, dB	−32.37 ± 4.91	−32.41 ± 3.73	16	−1.4679	0.16	**0.87**	−31.26 ± 4.87	−32.49 ± 4.99
V_{max}, μV	280.7 ± 102.1	291 ± 114.4	16	−0.0547	0.95	**0.75**	292.0 ± 28.2	279.7 ± 106.4
OCT CRT, μm	179.2 ± 35.3	175.8 ± 34.1	16	−0.3861	0.70	**0.84**	188.6 ± 54	179.1 ± 34.4
OCT category (n for each group)	5/13/6/7/3	5/13/6/7/3					0/3/1/0/0	5/10/5/7/3
Foveal hypoplasia present (n)	29	28					2	27

Because the iACHM group was too small, statistical comparison could not be performed; therefore, only mean ± SD is given for test results. Although contrast sensitivity and MP1 mean sensitivity seemed higher in iACHM, other test results did not differ. Furthermore, the SQ was flatter, but still within the limits for ACHM patients. df, degree of freedom; MP1, micropermetry; SQ, slope quotient on anomaloscope examination. Bold numbers indicate strong correlation.

** Indicate statistically significant P values at $P < 0.01$.

Table 3. Results of the CCT Showing the Color Discrimination Thresholds of Four Patients, as Determined by the Trivector Test

	Left Eye			Right Eye		
Patient No.	**Protan**	**Deutan**	**Tritan**	**Protan**	**Deutan**	**Tritan**
RD026	1100	1100	1100	1100	1100	1100
RD027	1100	1100	1100	1100	1100	1100
RD031	654	1030	1100	815	1100	1100
RD032	661	57	914	797	858	639

Numbers refer to vector length of discrimination along the protan, deutan, and tritan axis, in relative units in color space. With one exception (RD032, where discrimination along the deutan axis was normal), color discrimination was severely reduced in all patients and along all chromatic axes.

logMar), and mean contrast sensitivity was 1.21 ± 0.2 logCS (range, 0.75–1.5 logCS). The detailed clinical findings of patients are listed in Table 2.

Color vision was tested in two different setups in every patient. The Rayleigh anomaloscope matches were consistent with a rod-dominated function in every patient, and the average slope (SQ) of the decrease of the yellow half-field matched by the patient for equal luminance from the green to the red region was –1.6 ± 0.27 (range, –1.09 to –2.04). Some heterogeneity in the slopes could be detected; however, all were within the limits ascertained in ACHM patients by Pinckers.[34] The color confusion index (CCI) of the Roth 28 Hue saturated test was 5.22 ± 0.58 (range, 3.89–6.44), with an average angle of –59.22 ± 21.8° (range, 43.5° to –85.4°), also referring to extreme scotopization.[35] Both tests could reveal the defects in color discrimination; however, a correlation in performance of the two tests could not be observed (Table 2).

Table 3 shows the color discrimination thresholds of four patients, as determined by the Trivector test. Numbers refer to vector length of discrimination along the protan, deutan, and tritan axess, in relative units in color space. With one exception (RD032, where discrimination along the deutan axis was normal), color discrimination was severely impaired in all patients and along all chromatic axes. When comparing discrimination performance along the different axes, no differences were observed. Although only a few *CNGA3*-ACHM patients could be measured with CCT, this test seemed to be the most specific one to describe color confusions (Supplementary Fig. S1).

Although mean contrast sensitivity, SQ, and CCI did not show any correlation with age, or with each other, mean contrast sensitivity and BCVA did correlate (Table 4). Furthermore, we observed a tendency of weak improvement in BCVA with age ($P = -0.40$); also, kinetic visual field (VF) tests were performed better in older patients (VF area for target III4e: 10651.16 ± 2721.35 deg^2; range, 678.1–14835.3 deg^2). Patients with better VF areas and higher central light sensitivity in static perimetry tests (mean, 16.34 ± 9.57 dB; range, –2° to 30°) presented with better BCVA ($P = -0.33$ and $P = -0.42$, respectively).

Microperimetry indicated an overall lower retinal sensitivity within 20° of the visual field (mean sensitivity, 15.08 ± 2.37 dB; range, 10.17–19.46 dB), and mean fixation stability (BCEA) was 9.23 ± 8.23° (range, 2.12°–42.22°). (Results of MP1 measurements were compared with normal values of Midena et al.[36]) Interestingly, no correlations could be observed with results of other psychophysical tests discussed above or with age (Table 5).

Dark adaptation thresholds were measured with the FST test with two chromatic stimuli: (1) short wavelength stimuli (FST blue) resulted in a mean threshold of –56.17 ± 5.85 dB (range, –35.51 to –65.91 dB); and (2) threshold for long wavelength stimuli (FST red) was –32.37 ± 4.91 dB (range, –14.59 and –38.32 dB). Both FST blue and FST red, which are supposed to represent rod and cone dark adaptation thresholds, respectively,[28,29] were nearly normal (normal range for FST blue: –60.2 ± 6.4 dB; for FST red: –35.7 ± 3.3 dB); FST blue and FST red thresholds showed a strong correlation with each other and a weak correlation with the kinetic visual field areas. A correlation with other psychophysical parameters could not be observed (Table 5).

Electrophysiologic Results

In the electrophysiological examinations (Fig. 2), photopic responses were nondetectable in cACHM patients, but residual cone responses could be observed in the iACHM patients (in four cases, remaining responses only at 31-Hz flicker stimulus, in one patient, described above, responses for single flash recordings were detectable as well). Although ISCEV rod response (dark-adapted 0.01 ERG) amplitudes and implicit times were within normal limits, combined rod and cone (dark-adapted 3.0 ERG) response a-wave and b-wave amplitudes were on the lower limit of normal values, and implicit times of the b-waves were markedly delayed (Fig. 3; Supplementary Table S1). As a consequence of altered photoreceptor

Table 4. Correlation Between Parameters Regarding Central Retinal Function and Morphology (Data Given in the Table Refer to Pearson Correlation)

Clinical Parameters	**BCVA, logMAR**	**Contrast Sensitivity, logCS**	**Color Confusion, CCI**	**Anomaloscope Slope, SQ**	**OCT CRT, µm**	**Age, y**
BCVA, logMAR						
Contrast sensitivity, logCS	**−0.58****					
Color confusion, CCI	0.17	−0.29				
Anomaloscope slope, SQ	0.24	−0.21	0.21			
OCT CRT, µm	0.17	−0.02	0.04	0.31		
Age, y	**−0.40***	0.25	0.21	0.22	0.02	

Interestingly, only BCVA and mean contrast sensitivity showed a good correlation, other parameters did not correlate with each other or with age. Furthermore, we observed a tendency of weak improvement in BCVA with age. Bold values indicate parameters showing correlation, where * indicates weak correlation, ** indicates good correlation.

Table 5. Correlation Between Parameters Regarding General Retinal Function (Data Given in the Table Refer to Spearman Correlation)

Clinical Parameters	FST Blue, dB	FST Red, dB	V_{max}, μV	MP1 Mean Sensitivity, dB	Kinetic VF III4e, deg^2	Age, y
FST blue, dB						
FST red, dB	**0.82****					
V_{max}, μV	−0.1	−0.12				
MP1 mean sensitivity, dB	−0.0012	−0.13	0.16			
Kinetic VF III4e, deg^2	−0.27	**−0.34***	−0.06	0.26		
Age, y	−0.04	−0.17	−0.11	0.16	0.2	

Only results of the FST blue and red tests showed a strong correlation; other parameters seemed to be independent from each other. Bold values indicate parameters showing correlation, where * indicates weak correlation, ** indicates good correlation.

functions, oscillatory potentials were markedly attenuated (Fig. 2B).

In the stimulus–response function of the scotopic ERG, V_{max} (mean, 280.7 ± 102.1 μV) was significantly below normal values ($P < 0.05$). In contrast, slope (n mean, 1.01 ± 0.24) and semisaturation intensity (log$K$ mean, −3.0 ± 0.3 log cd.s/m^2) were found to be within normal limits (Fig. 4).

Due to nystagmus and marked photophobia, multifocal ERG (mfERG) recordings could be performed only in 14 patients; however, reproducible responses were only detected in 1 iACHM patient (RD036), whose overall results were strikingly better.

The psychophysical and electrophysiologic findings were also analyzed for intraindividual differences. For most parameters, a good correlation between the right and left eye and between the dominant and nondominant eye could be detected (Table 2; Supplementary Table S2). The CCI values of the Roth 28 Hue test were not consistent between eyes; however, a difference in mean values was not observed.

Furthermore, we found significantly better BCVA and contrast sensitivity parameters in the dominant eye ($P = 0.0069$ and $P = 0.0076$, respectively; paired t-test). Other psychophysical or electrophysiologic results did not differ between the dominant and nondominant eye, nor between the right and left eye (Table 2; Supplementary Table S2). Furthermore, no striking differences in functional or electrophysiologic results between iACHM and cACHM patients could be observed, although contrast sensitivity and MP1 mean sensitivity seemed higher in iACHM and the slope on anomaloscope measurements was flatter, but still within the limits (Table 2). (A detailed statistical analysis is not possible due to the small number of iACHM patients.)

Morphologic Results

On the morphologic level, SD-OCT examination showed the following: (1) no specific changes in 14.7%, (2) EZ disruption at the fovea in 38.2%, (3) absent EZ in 17.7%, (4) a HRZ in 20.5%, and (5) outer retinal atrophy including RPE loss in 8.9% of all cases. Mean central retinal thickness was 179.2 ± 35.3 μm (range, 69–239 μm) for all patients. Age distribution was very similar among categories; however, the few patients showing outer retinal atrophy and RPE loss, resulting in marked thinning of the fovea, were all above 37 years (Table 6). Further noticeable differences regarding retinal function could not be detected among the OCT categories.

Foveal hypoplasia was found in 29 patients (85%); however, no correlation with central visual function could be observed

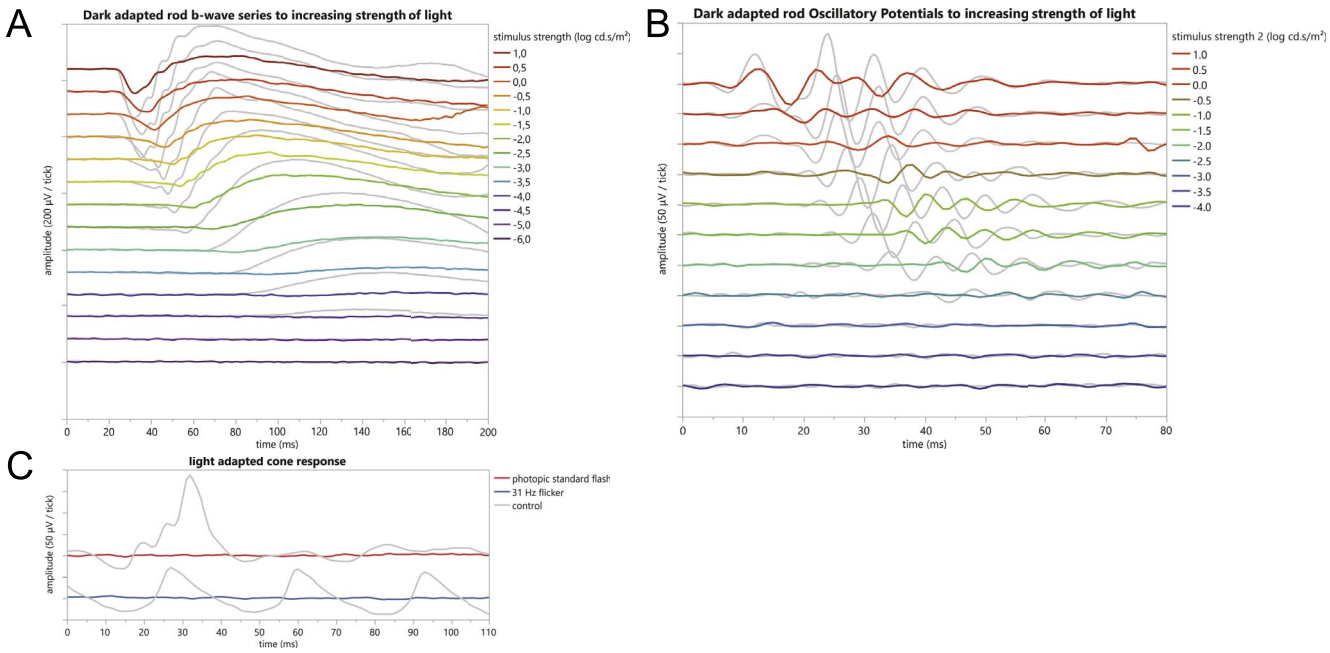

Figure 2. Electroretinography results from a representative ACHM patient (RD020). (**A**) Reduced scotopic responses, (**B**) attenuated oscillatory potentials to increasing stimulus intensities, and (**C**) diminished photopic responses were typical findings. The *gray curves* show results of a normal person.

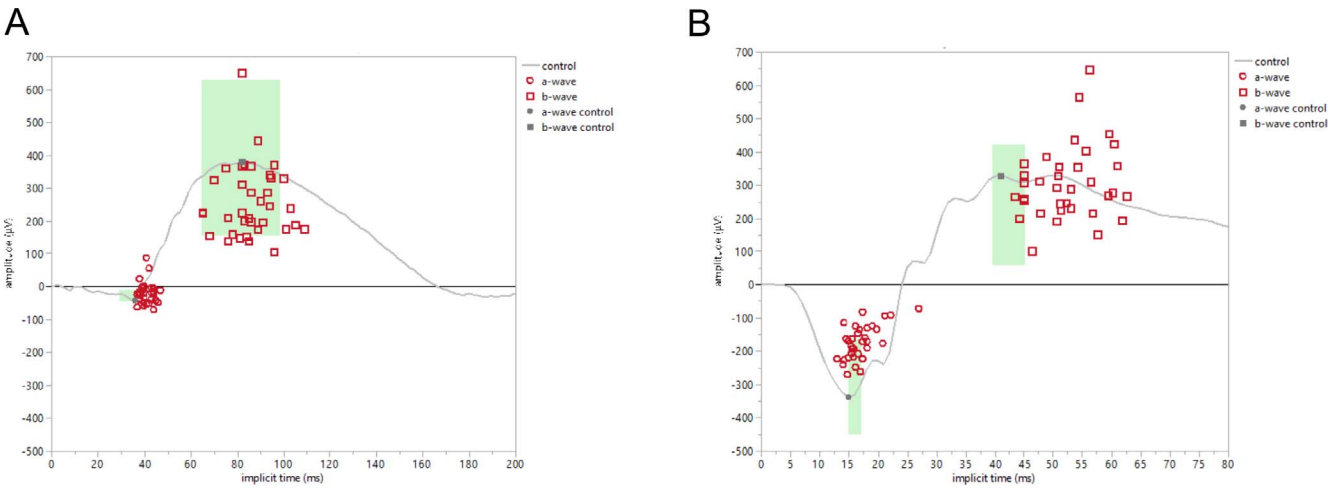

Figure 3. ISCEV dark-adapted 0.01 (**A**) and 3.0 ERG responses (**B**). Although rod response amplitudes and implicit times were within normal limits (**A**), combined rod and cone response a-wave and b-wave amplitudes were on the lower limit of normal values and implicit times of b-waves were markedly delayed (**B**). The *green-shaded boxes* refer to the normal range (5%–95% confidence intervals).

(BCVA was 0.78 ± 0.12 and 0.8 ± 0.12 logMAR; contrast sensitivity was 1.22 ± 0.18 and 1.14 ± 0.31 logCS; and CCI was 5.20 ± 0.56 and 5.29 ± 0.77 in eyes with and without foveal hypoplasia, respectively). Detailed statistical analysis was not possible due to the small number of eyes without foveal hypoplasia.

Fundus autofluorescence imaging also showed variable pathologic features, depending on the severity of morphologic changes observed in SD-OCT. Foveal hyperfluorescence was detected in patients without specific changes or with only intermittent inner segment (Ise) disruption on OCT. In patients with disrupted or even absent, EZ reduced foveal AF could be detected; in some cases, they were surrounded by a zone with increased AF. The area of reduced AF appeared more sharply demarcated in the cases where a HRZ on OCT was observed. In the most severe cases, revealing outer retinal and RPE atrophy, foveal AF was absent. Exemplary morphologic results are presented in Figure 5, and the functional findings of each OCT group are listed in Table 6.

Discussion

Our study applying extended clinical protocols showed that even in the genetically defined group of *CNGA3*-ACHM patients, no specific correlations regarding allelic mutations, function, and morphology could be observed. The severity of morphologic and functional changes also lacked a robust association with age. These findings further support and are in line with the results of other reported ACHM groups.[15,37,38]

To further address the question of validity and predictive value of functional in vitro data, we also looked at the clinical findings in regard of remaining function suspected on the basis of genetic mutations. All of our iACHM patients revealed mutations that were shown to yield residual channel function in functional in vitro experiments.[33,39–42] However, in some cases, no cone function was detectable despite residual channel function, albeit with deviant functional properties, in heterologous expression systems.[39–42] Therefore, we can assume that the specific genetic mutation cannot reliably predict the clinical phenotype.

Furthermore, eight ACHM patients with the same homozygous mutation (c.847C>T;p.R283W) were further analyzed as a subgroup. All of these patients (age between 7–43 years) were clinically complete achromats, and foveal hypoplasia was observed in both eyes in every case; however, functional and other morphologic results did not show any differences in comparison to the group averages. Retinal atrophy and loss of RPE was not detected in any of these cases, but it might be explained with the younger ages of patients in this subgroup.

A further purpose of the study was to experience which clinical tests will be most suitable in the interventional study phase. There were some interesting observations regarding function. The performance on psychophysical tests in younger patients, especially in visual acuity and perimetry, was strongly influenced by photophobia. Patients under 18 years showed a tendency to slightly worse BCVA and concentric narrowing of the visual field; the latter was not seen in any of the older patients. This phenomenon might be explained with better compliance, longer adaptation to the condition or loss of photoreceptors with age, and the concomitantly reduced photophobia that possibly enables improved test performance over the years in adult patients.

Photophobia is indeed a limiting factor in several functional and morphologic tests; however, measuring the eventual change in photoaversion could also be an important parameter in treatment studies, as also suggested by Zelinger et al.[43] Recently, Aguilar et al. demonstrated the usefulness of the ocular photosensitivity analyzer in ACHM patients (Aguilar M et al. *IOVS* 2016;136:ARVO E-Abstract 622). This test could be considered for future interventional studies; however, further validation and larger patient groups are needed.

Color discrimination is attractive for a trial aimed at modifying and possibly enhancing cone function and could be an important metric in a gene therapy trial.[44,45] Although the Rayleigh anomaloscope is indeed a suitable test to clinically diagnose ACHM and determination of SQ makes it reproducible and therefore appropriate for follow-up purposes, an even more specific characterization of color vision regarding residual cone function (protan, deutan, or tritan) could be achieved with the CCT. Therefore, this test could suitably describe functional changes in color perception and should be considered as an additional test when planning interventional studies. The use of the Rayleigh anomaloscope and CCT have already been demonstrated by Zein et al.[44] in a human *CNGB3*-ACHM trial with ciliary neurotrophic factor (CNTF) and by Mancuso et al.[45] in dichromatic nonhuman primates after gene therapy.

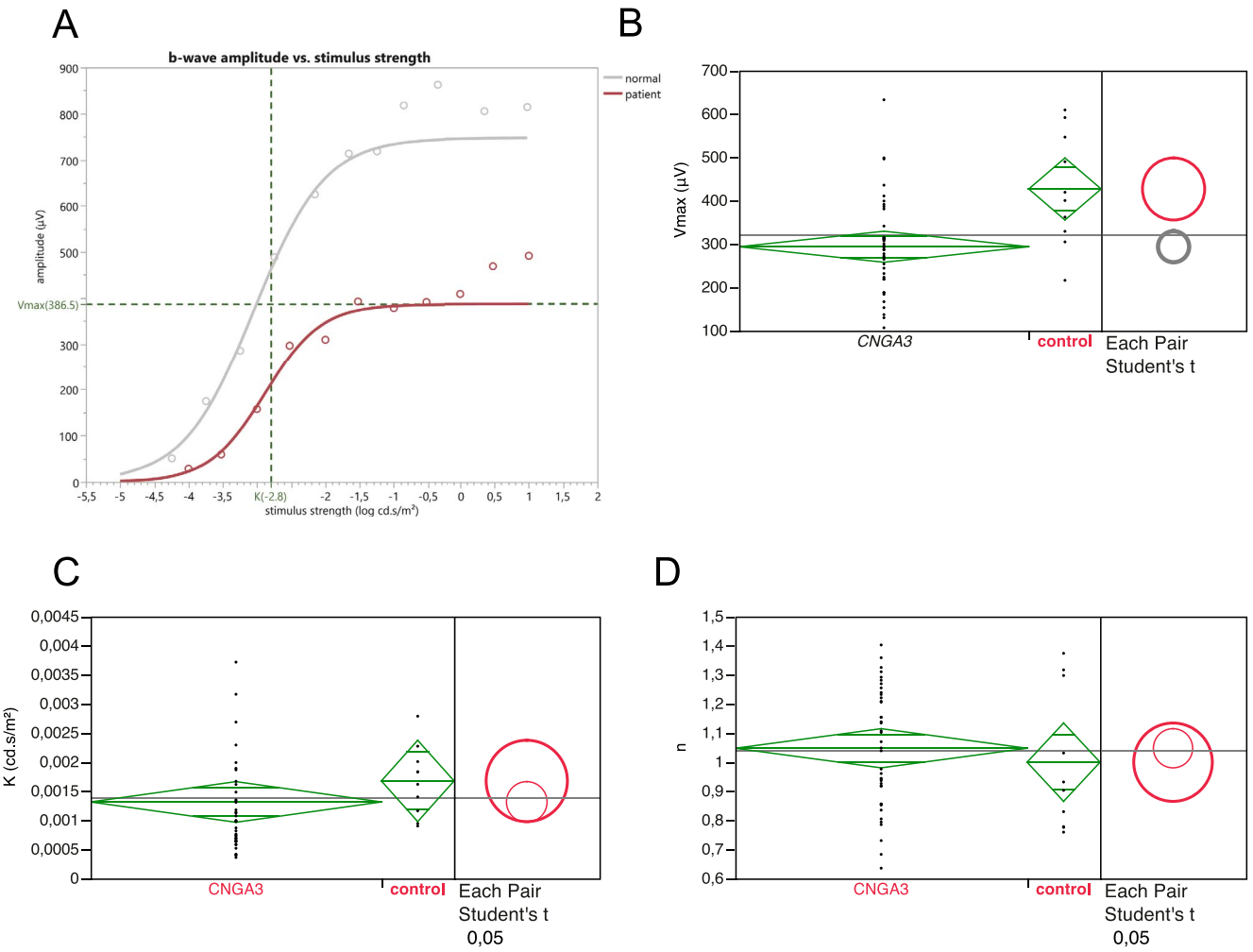

Figure 4. Intensity–response function kinetics under scotopic conditions (**A**) of a representative patient (RD020: *red line*; normal person: *gray line*). V_{max} (maximum b-wave amplitude), n (slope-related exponent), and K (flash intensity required for semisaturation) were calculated for ACHM patients. The estimated V_{max} was lower in patients (**B**), but parameters K (**C**) and n (**D**) were found to be within normal limits compared to control subjects. The mean values of each parameter of ACHM patients and control subjects are represented with comparison circles. *Circles* for means that do not intersect are significantly different (V_{max}), whereas *nested circles* mean no statistical difference (n and K). Notice the deviating data points of the ACHM patient above 0.5 log cd.s/m^2 stimulus intensity (**A**), which might be explained due to altered crosstalk between the rod and cone systems at the photoreceptoral or postreceptoral levels.

In contrast, when measuring dark adaptation thresholds, we found the FST measurements not reliable enough to separately investigate rod and cone function. Both FST blue and red tests, which supposedly represent rod and cone dark adaptation thresholds,[28,29] respectively, were nearly normal. This was a surprising result, because we expected to see good function of the rods in response to blue stimuli but altered cone thresholds for the red stimuli. The nearly normal thresholds seen for both chromatic stimuli could be explained by the overlapping spectral sensitivity curves of rods and cones in the long wavelength spectral region.[46] Although the threshold of rod and cone vision for blue FST stimuli (wavelength 465 nm) are very different, the threshold for the long wave stimulus (635 nm) is almost equal for rods and longwave length-sensitive

Table 6. Comparison of Functional and Morphologic Results Between OCT Categories

Clinical Parameters	1, $n = 5$	2, $n = 13$	3, $n = 6$	4, $n = 7$	5, $n = 3$
Age, y	33.6 ± 11.1	32.4 ± 13.7	38 ± 14.6	32.3 ± 16.6	**43.3 ± 7.7**
BCVA, logMAR	0.78 ± 0.17	0.81 ± 0.09	0.73 ± 0.08	0.78 ± 0.17	0.77 ± 0.11
Contrast sensitivity, logCS	1.2 ± 0.18	1.16 ± 0.25	1.27 ± 0.08	1.32 ± 0.19	1.15 ± 0.17
Color confusion, CCI	5.22 ± 0.43	5.49 ± 0.52	4.98 ± 0.89	4.89 ± 0.31	5.19 ± 0.52
Anomaloscope slope, SQ	−1.35 ± 0.3	−1.57 ± 0.3	−1.74 ± 0.22	−1.72 ± 0.16	−1.63 ± 0.14
OCT CRT, µm	205.6 ± 22.8	183.1 ± 26.5	166.6 ± 26.1	192.1 ± 30.1	**112.3 ± 38.1**

Striking differences regarding retinal function could not be detected among the OCT categories. Also, age distribution was very similar among categories; however, the few patients showing outer retinal atrophy and RPE loss (resulting in thinning of the fovea) were all greater than 37 years of age. Bold numbers indicate parameters with statistical relevance.

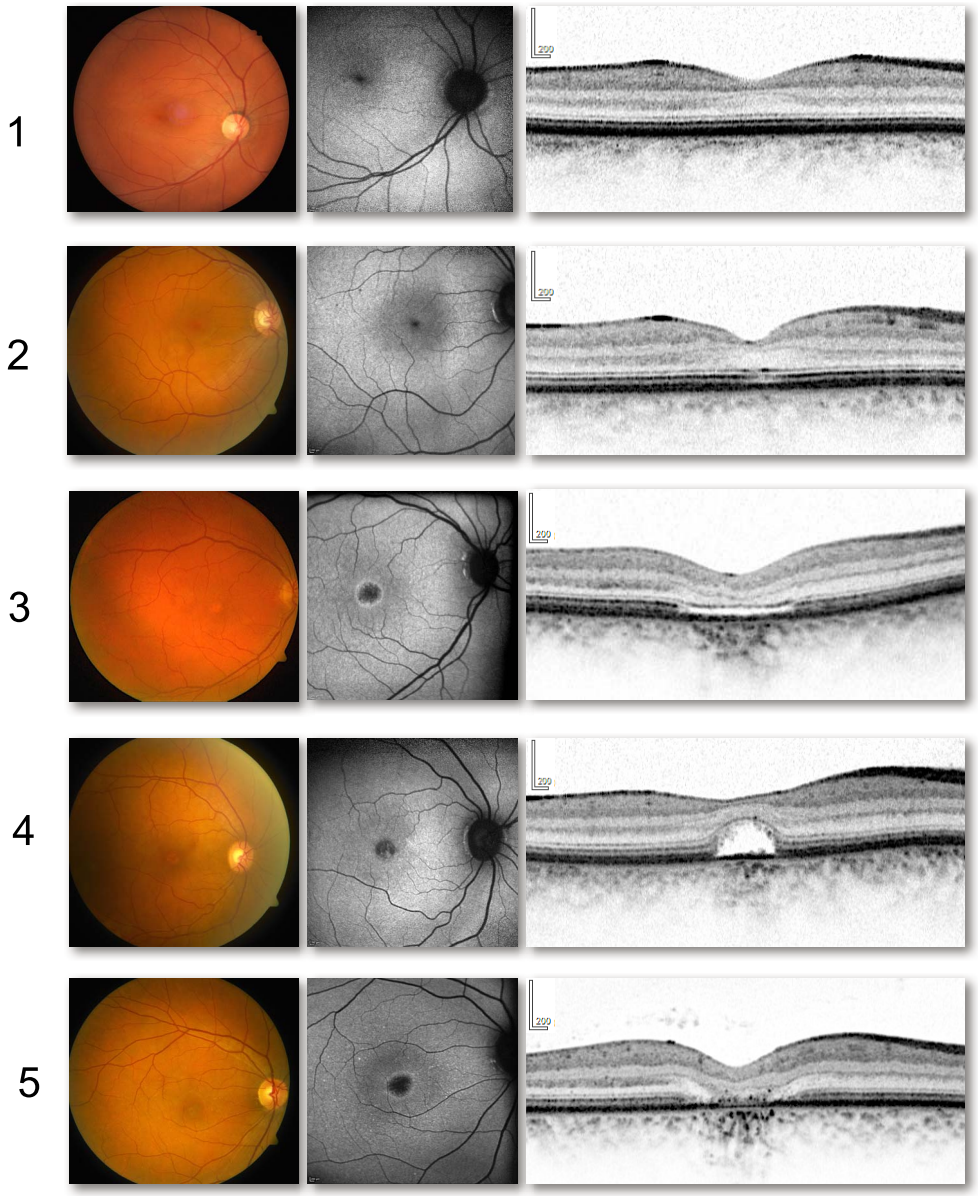

Figure 5. Representative fundus photographs, FAF, and OCT images for each group categorized by OCT characteristics. (1) No specific changes in 14.7%, (2) EZ disruption at the fovea in 38.2%, (3) absent EZ in 17.7%, (4) a hyporeflective zone (HRZ) in 20.5%, and (5) outer retinal atrophy including RPE loss was seen in 8.9% of all cases. Foveal hypoplasia was found in 29 patients (85%); however, no correlation with visual function could be observed.

cones. Therefore, the FST test with long wavelength light cannot reliably differentiate between rod and cone function, especially given the range of variations even within normal values. Therefore, we consider it valid to assume that the threshold for long wavelength stimuli was determined by the rods in our patients. The nearly normal responses to red stimuli then could originate from functioning rods. In conclusion, FST in the present form should not be considered to observe treatment efficacy for cone function; however, for safety aspects, rod function could still be monitored with the help of this method.

Cone-mediated ERG responses are mostly nonrecordable in ACHM,[1–3,47] although anomalies in rod pathway signaling and deficits in postreceptor responses have also been reported, even though the genetic defect is cone specific. This could reflect either a smaller number of rods, shorter rod outer segments, and/or altered rod circuitry.[3,43] Furthermore, in a *cnga3*$^{-/-}$ mouse model, anomalous synapses between rods and cone bipolar cells have also been documented.[48] Our data also showed alterations of the scotopic ERG. Because conventional gene therapy applying subretinal delivery of the vector will only treat a small area of the retina, no marked improvement of cone function on full-field ERG measurements should be expected. However, again for safety reasons concerning the rod system, electrophysiology remains inevitable, but one should keep in mind that alterations in rod pathway signaling occur.[3,43]

Standard mfERG recordings were found to be difficult to perform due to photophobia and nystagmus, which is a further limiting factor when it comes to functional and morphologic characterization. Especially, the quality and reliability of MP-1 and mfERG measurements have unstable fixation and uncon-

trollable eye movements, but also OCT and AO measurements can become challenging. Further technical improvement with an eye tracking system fast enough might compensate nystagmus or unstable fixation better and could improve the quality of a fundus-controlled mfERG measurement, whereas microperimetry might benefit from a specific, examiner-determined pattern with less points measured.

The potential of pupillography has been examined in several interventional trials, which holds promise for an alternative objective measurement of efficacy. We developed a protocol for chromatic pupillography to be used for the objective assessment of efficacy of gene therapy or other innovative interventions in ACHM. The results are reported separately by Lisowska et al. (manuscript in preparation).

Several clinical studies in recent years have investigated outer retinal architecture and foveal morphology in detail by using high-resolution OCT and AO[15–17,26,49–51] in ACHM. The macular appearances in OCT can either show normal lamination or variable degrees of disruption of the photoreceptor layers and loss of RPE. In our patient group, we also used the categorization previously described by Sundaram et al.[15] and found very similar results, even though the genetic basis of disease in our study was more homogeneous. However, a great variability in morphologic findings was observed in our cohort of patients. Notably, there is some disagreement regarding the progressive nature of morphologic changes in ACHM in the literature: Thiadens et al.[17] concluded that ACHM is not a stationary disease, but a disorder that shows progressive loss of cone photoreceptors. Thomas et al.[16] also showed progressive longitudinal changes in retinal morphology in children and described an interesting OCT sign, a hyperreflective zone, which appears to be the precursor of the hyporeflective zone seen in later ages. On the contrary, Genead et al.[26] provided evidence that cone loss is not age dependent. In our study, in patients with defined *CNGA3*-ACHM, a clear age-dependent cone loss was not observed, and most of the patients fell into OCT categories 1 to 4, where age distribution was very similar. Only a few cases showed RPE loss, outer retinal atrophy, and therefore reduced central retinal thickness (CRT), but in fact, all patients were older than 37 years of age.

With the technology of AO, Carroll et al.[20] observed a severely disrupted cone mosaic in the fovea and parafoveal area of a single patient with mutations in *CNGB3*. Genead et al.[26] reported residual cone structures in all nine patients carrying mutations either in *CNGA3* or *CNGB3*, although the majority of cones had reduced reflectance. Dubis et al.[21] also reported reduced numbers and variable reflectivity of cones and suggest that reflectivity could be a more powerful AO metric for interventional studies, as increased numbers cones could not be expected due to treatment. Very recently, Langlo et al.[52] reported on the residual foveal cone structure in 26 *CNGB3*-ACHM patients and concluded that a more severe OCT phenotype may be evidence for a low cone density, but a less disrupted OCT grade could correspond to either a high or low cone density. The presence of remnant inner segment cone structure indicates that disruptions in the EZ do not necessarily correlate to the degree of photoreceptor loss in the foveal region. Retinas with larger numbers of cone inner segments may have a greater therapeutic potential than individuals with fewer remnant cones, although the organization of the residual cones should also be taken into consideration.[52]

Achromatopsia can probably be best described as a functionally stationary disorder with a slow degeneration of the nonfunctional cone photoreceptors. It has long been considered an ideal target for gene therapy,[25,53–57] based on the observation, that, in contrast to other progressive retinal dystrophies, the nonfunctioning cone photoreceptors seem to be largely and longer preserved, suggesting a wider therapeutic window.[26,49–52] The positive effects observed in preclinical studies on animal models of ACHM hold promise for future therapeutic approaches in human patients,[25,45,53–57] but it still remains uncertain what functional changes can be expected after treatment. Therefore, detailed clinical characterization and long-term observations, including psychophysiologic and objective measurements, in preparation of an interventional study have a key role in the evaluation of therapeutic effects. Because expectations on functional changes are rather incalculable,[58,59] both subjective and objective measurement results, as clinical end points, should be considered. Burton et al.[58] suggested that ACHM leads to atypical development of cortical vision, highlighting the need to better understand the potential for further reorganization of cortical visual processing. In addition, it would be interesting to determine whether individuals with greater numbers of foveal cones showed the same degree of cortical reorganization, as this is a potential complication in the pursuit of restoring cone vision in patients with ACHM.[52,57,58]

Because no clear association between retinal structure and function or CNGA3 genotype is obvious, it also needs to be elucidated what other educational, environmental, or psychological factors could have an influence on coping with the disease. However, this also suggests that no therapeutic window can be defined per se, and not age, but more likely function and morphology, will be pivotal in choosing eligible patients for interventional studies. Beyond that, there is a further need to study the ability of the visual system to respond to the novel input to establish the most appropriate protocols to identify suitable patients and follow the therapeutic effect.

Acknowledgments

The RD-Cure project is funded by the Tistou and Charlotte Kerstan Foundation.

Disclosure: **D. Zobor**, None; **A. Werner**, None; **F. Stanzial**, None; **F. Benedicenti**, None; **G. Rudolph**, None; **U. Kellner**, None; **C. Hamel**, None; **S. Andréasson**, None; **G. Zobor**, None; **T. Strasser**, None; **B. Wissinger**, None; **S. Kohl**, None; **E. Zrenner**, None

References

1. Kohl S, Hamel C. Clinical utility gene card for: achromatopsia—update 2013. *Eur J Hum Genet*. 2013;21.
2. Kohl S, Jägle H, Wissinger B. Achromatopsia. In: *GeneReviews*. Pagon RA, Adam MP, Ardinger HH, eds. Available at: http://www.ncbi.nlm.nih.gov/books/NBK1418/.
3. Moskowitz A, Hansen RM, Akula JD, Eklund SE, Fulton AB. Rod and rod-driven function in achromatopsia and blue cone monochromatism. *Invest Ophthalmol Vis Sci*. 2009;50:950–958.
4. Thiadens AA, Slingerland NW, Roosing S, et al. Genetic etiology and clinical consequences of complete and incomplete achromatopsia. *Ophthalmology*. 2009;116:1984–1989, e1981.
5. Kohl S, Marx T, Giddings I, et al. Total colour-blindness is caused by mutations in the gene encoding the alpha-subunit of the cone photoreceptor cGMP-gated cation channel. *Nat Genet*. 1998;19:257–259.
6. Kohl S, Baumann B, Broghammer M, et al. Mutations in the CNGB3 gene encoding the beta-subunit of the cone photoreceptor cGMP-gated channel are responsible for achromatopsia (ACHM3) linked to chromosome 8q21. *Hum Mol Genet*. 2000;9:2107–2116.
7. Kohl S, Varsanyi B, Antunes GA, et al. CNGB3 mutations account for 50% of all cases with autosomal recessive achromatopsia. *Eur J Hum Genet*. 2005;13:302–308.

8. Kohl S, Baumann B, Rosenberg T, et al. Mutations in the cone photoreceptor G-protein alpha-subunit gene GNAT2 in patients with achromatopsia. *Am J Hum Genet*. 2002;71:422–425.
9. Grau T, Artemyev NO, Rosenberg T, et al. Decreased catalytic activity and altered activation properties of PDE6C mutants associated with autosomal recessive achromatopsia. *Hum Mol Genet*. 2011;20:719–730.
10. Thiadens AA, den Hollander AI, Roosing S, et al. Homozygosity mapping reveals PDE6C mutations in patients with early-onset cone photoreceptor disorders. *Am J Hum Genet*. 2009;85:240–247.
11. Kohl S, Coppieters F, Meire F, et al. A nonsense mutation in PDE6H causes autosomal-recessive incomplete achromatopsia. *Am J Hum Genet*. 2012;91:527–532.
12. Wissinger B, Gamer D, Jagle H, et al. CNGA3 mutations in hereditary cone photoreceptor disorders. *Am J Hum Genet*. 2001;69:722–737.
13. Kohl S, Zobor D, Chiang WC, et al. Mutations in the unfolded protein response regulator ATF6 cause the cone dysfunction disorder achromatopsia. *Nat Genet*. 2015;47:757–765.
14. Thiadens AA, Roosing S, Collin RW, et al. Comprehensive analysis of the achromatopsia genes CNGA3 and CNGB3 in progressive cone dystrophy. *Ophthalmology*. 2010;117:825–830, e821.
15. Sundaram V, Wilde C, Aboshiha J, et al. Retinal structure and function in achromatopsia: implications for gene therapy. *Ophthalmology*. 2014;121:234–245.
16. Thomas MG, McLean RJ, Kohl S, Sheth V, Gottlob I. Early signs of longitudinal progressive cone photoreceptor degeneration in achromatopsia. *Br J Ophthalmol*. 2012;96:1232–1236.
17. Thiadens AA, Somervuo V, van den Born LI, et al. Progressive loss of cones in achromatopsia: an imaging study using spectral-domain optical coherence tomography. *Invest Ophthalmol Vis Sci*. 2010;51:5952–5957.
18. Aboshiha J, Dubis AM, Cowing J, et al. A prospective longitudinal study of retinal structure and function in achromatopsia. *Invest Ophthalmol Vis Sci*. 2014;55:5733–5743.
19. Scoles D, Sulai YN, Langlo CS, et al. In vivo imaging of human cone photoreceptor inner segments. *Invest Ophthalmol Vis Sci*. 2014;55:4244–4251.
20. Carroll J, Choi SS, Williams DR. In vivo imaging of the photoreceptor mosaic of a rod monochromat. *Vision Res*. 2008;48:2564–2568.
21. Dubis AM, Cooper RF, Aboshiha J, et al. Genotype-dependent variability in residual cone structure in achromatopsia: towards developing metrics for assessing cone health. *Invest Ophthalmol Vis Sci*. 2014;55:7303–7311.
22. Michalakis S, Muhlfriedel R, Tanimoto N, et al. Restoration of cone vision in the CNGA3-/- mouse model of congenital complete lack of cone photoreceptor function. *Mol Ther*. 2010;18:2057–2063.
23. Pang JJ, Alexander J, Lei B, et al. Achromatopsia as a potential candidate for gene therapy. *Adv Exp Med Biol*. 2010;664:639–646.
24. Carvalho LS, Xu J, Pearson RA, et al. Long-term and age-dependent restoration of visual function in a mouse model of CNGB3-associated achromatopsia following gene therapy. *Hum Mol Genet*. 2011;20:3161–3175.
25. Michalakis S, Mühlfriedel R, Tanimoto N, et al. Restoration of cone vision in the CNGA3-/- mouse model of congenital complete lack of cone photoreceptor function. *Mol Ther*. 2010;18:2057–2063.
26. Genead MA, Fishman GA, Rha J, et al. Photoreceptor structure and function in patients with congenital achromatopsia. *Invest Ophthalmol Vis Sci*. 2011;52:7298–7308.
27. Regan BC, Reffin JP, Mollon JD. Luminance noise and the rapid determination of discrimination ellipses in colour deficiency. *Vision Res*. 1994;34:1279–1299.
28. Klein M, Birch DG. Psychophysical assessment of low visual function in patients with retinal degenerative diseases (RDDs) with the Diagnosys full-field stimulus threshold (D-FST). *Doc Ophthalmol*. 2009;119:217–224.
29. Collison FT, Fishman GA, McAnany JJ, Zernant J, Allikmets R. Psychophysical measurement of rod and cone thresholds in stargardt disease with full-field stimuli. *Retina*. 2014;34:1888–1895.
30. McCulloch DL, Marmor MF, Brigell MG, et al. ISCEV Standard for full-field clinical electroretinography (2015 update). *Doc Ophthalmol*. 2015;130:1–12.
31. Hood DC, Bach M, Brigell M, et al. ISCEV standard for clinical multifocal electroretinography (mfERG) (2011 edition). *Doc Ophthalmol*. 2012;124:1–13.
32. Thomas MG, Kumar A, Mohammad S, et al. Structural grading of foveal hypoplasia using spectral-domain optical coherence tomography a predictor of visual acuity? *Ophthalmology*. 2011;118:1653–1660.
33. Muraki-Oda S, Toyoda F, Okada A, et al. Functional analysis of rod monochromacy-associated missense mutations in the CNGA3 subunit of the cone photoreceptor cGMP-gated channel. *Biochem Biophys Res Commun*. 2007;362:88–93.
34. Pinckers A. Anomaloscope examination: scotopization (the luminance fall). *Acta Ophthalmol Scand*. 1999;77:552–554.
35. Török B. WEB-based Scoring Software for the Farnsworth-Munsell 100-Hue, Roth 28-Hue, Farnsworth D-15, and the Lanthony D-15 Desaturated Color Tests (2014). Available at: http://www.torok.info/colorvision/.
36. Midena E, Vujosevic S, Cavarzeran F; Microperimetry Study Group. Normal values for fundus perimetry with the microperimeter MP1. *Ophthalmology*. 2010;117:1571–1576.
37. Aboshiha J, Luong V, Cowing J, et al. Dark-adaptation functions in molecularly confirmed achromatopsia and the implications for assessment in retinal therapy trials. *Invest Ophthalmol Vis Sci*. 2014;55:6340–6349.
38. Aboshiha J, Dubis AM, Cowing J, et al. A prospective longitudinal study of retinal structure and function in achromatopsia. *Invest Ophthalmol Vis Sci*. 2014;55:5733–5743.
39. Reuter P, Koeppen K, Ladewig T, Kohl S, Baumann B, Wissinger B; Achromatopsia Clinical Study Group. Mutations in CNGA3 impair trafficking or function of cone cyclic nucleotide-gated channels, resulting in achromatopsia. *Hum Mutat*. 2008;29:1228–1236.
40. Koeppen K, Reuter P, Kohl S, Baumann B, Ladewig T, Wissinger B. Functional analysis of human CNGA3 mutations associated with colour blindness suggests impaired surface expression of channel mutants A3(R427C) and A3(R563C). *Eur J Neurosci*. 2008;27:2391–2401.
41. Matveev AV, Fitzgerald JB, Xu J, Malykhina AP, Rodgers KK, Ding XQ. The disease-causing mutations in the carboxyl terminus of the cone cyclic nucleotide-gated channel CNGA3 subunit alter the local secondary structure and interfere with the channel active conformational change. *Biochemistry*. 2010;49:1628–1639.
42. Tränkner D, Jägle H, Kohl S, et al. Molecular basis of an inherited form of incomplete achromatopsia. *J Neurosci*. 2004;24:138–147.
43. Zelinger L, Cideciyan AV, Kohl S, et al. Genetics and disease expression in the CNGA3 form of achromatopsia: steps on the path to gene therapy. *Ophthalmology*. 2015;122:997–1007.
44. Zein WM, Jeffrey BG, Wiley HE, et al. CNGB3-Achromatopsia Clinical Trial With CNTF: diminished rod pathway responses with no evidence of improvement in cone function. *Invest Ophthalmol Vis Sci*. 2014;55:6301–6308.

Investigative Ophthalmology & Visual Science

45. Mancuso K, Hauswirth WW, Li Q, et al. Gene therapy for red-green colour blindness in adult primates. *Nature*. 2009;461:784–787.
46. Stiles WS, Crawford H. The luminous efficiency of rays entering the eye pupil at different points. *Proc R Soc Lond*. 1933;112:428–450.
47. Zobor D, Zobor G, Kohl S. Achromatopsia: on the doorstep of a possible gene therapy. *Ophthalmic Res*. 2015;54:103–108.
48. Haverkamp S, Michalakis S, Claes E, et al. Synaptic plasticity in CNGA3(-/-) mice: cone bipolar cells react on the missing cone input and form ectopic synapses with rods. *J Neurosci*. 2006;26:5248–5255.
49. Abozaid MA, Langlo CS, Dubis AM, Michaelides M, Tarima S, Carroll J. Reliability and repeatability of cone density measurements in patients with congenital achromatopsia. *Adv Exp Med Biol*. 2016;854:277–283.
50. Thomas MG, Kumar A, Kohl S, Proudlock FA, Gottlob I. High-resolution in vivo imaging in achromatopsia. *Ophthalmology*. 2011;118:882–887.
51. Greenberg JP, Sherman J, Zweifel SA, et al. Spectral-domain optical coherence tomography staging and autofluorescence imaging in achromatopsia. *JAMA Ophthalmol*. 2014;132:437–445.
52. Langlo CS, Patterson EJ, Higgins BP, et al. Residual foveal cone structure in CNGB3-associated achromatopsia. *Invest Ophthalmol Vis Sci*. 2016;57:3984–3995.
53. Pang JJ, Deng WT, Dai X, et al. AAV-mediated cone rescue in a naturally occurring mouse model of CNGA3-achromatopsia. *PLoS One*. 2012;7:e35250.
54. Reicher S, Seroussi E, Gootwine E. A mutation in gene CNGA3 is associated with day blindness in sheep. *Genomics*. 2010;95:101–104.
55. Komaromy AM, Rowlan JS, Corr AT, et al. Transient photoreceptor deconstruction by CNTF enhances rAAV-mediated cone functional rescue in late stage CNGB3-achromatopsia. *Mol Ther*. 2013;21:1131–1141.
56. Schön C, Biel M, Michalakis S. Gene replacement therapy for retinal CNG channelopathies. *Mol Genet Genomics*. 2013;288:459–467.
57. Komaromy AM, Alexander JJ, Rowlan JS, et al. Gene therapy rescues cone function in congenital achromatopsia. *Hum Mol Genet*. 2010;19:2581–2593.
58. Burton E, Wattam-Bell J, Rubin G, et al. Dissociations in coherence sensitivity reveal atypical development of cortical visual processing in congenital achromatopsia. *Invest Ophthalmol Vis Sci*. 2016;57:2251–2259.
59. Baseler HA, Brewer AA, Sharpe LT, Morland AB, Jägle H, Wandell BA. Reorganization of human cortical maps caused by inherited photoreceptor abnormalities. *Nat Neurosci*. 2002;5:364–370.

Appendix

Members of the RD-Consortium are as follows: Karl Ulrich Barzt-Schmidt, Sylvia Bolz, Dominik Fischer, Susanne Kohl, Laura Kühlewein, Regine Mühlfriedel, Alex Ochakovski, Francois Paquet-Durand, Mathias Seeliger, Vithiyanjali Sothilingam, Marius Ueffing, Nicole Weisschuh, Bernd Wissinger, Ahmad Zhour, Ditta Zobor, Eberhart Zrenner (Centre for Ophthalmology, University of Tuebingen, Germany); Martin Biel, Stylianos Michalakis, Christian Schön (Department of Pharmacy - Center for Drug Research, Ludwig-Maximilians-Universität München, Germany); Nadine Kahle, Tobias Peters, Barbara Wilhelm (STZ eyetrial at the Centre for Ophthalmology, University of Tübingen, Germany); Steven Tsang (Department of Ophthalmology, Columbia University, New York, USA); Christian Johannes Glöckner (Deutsches Zentrum für Neurodegenerative Erkrankungen, Tuebingen, Germany). The clinical and genetic work was supported by Peggy Reuter, Ulrike Fuchs, Gudrun Haerer and Susanne Kramer.

Investigative Ophthalmology & Visual Science